communications biology

A Nature Portfolio journal

Article

https://doi.org/10.1038/s42003-025-07758-w

Measuring pH in insulin secretory granules by phasor-based fluorescence lifetime imaging of a genetically encoded sensor

Valentina De Lorenzi [1] ✉, Samuele Ghignoli [1], Mario Bernardi [1], Giulia Matteoli [1,5], Gianmarco Ferri[2], Barbara Storti[3], Ranieri Bizzarri [3,4] & Francesco Cardarelli [1] ✉

It is widely accepted that the pH of insulin granules is acidic, and that its active regulation during granule maturation plays a role in the process of insulin secretion by β-cells. Yet, a calibrated measurement of the absolute granule pH with organelle specificity is still lacking. To tackle this issue, we use the genetically encoded E^{1}GFP pH reporter inserted into the C-peptide of proinsulin and expressed in Insulinoma 1E cells. Following verification of correct targeting of the E^{1}GFP reporter in the insulin granules, phasor-based Fluorescence Lifetime Imaging Microscopy (FLIM) is applied to obtain a calibrated and probe-concentration-independent measurement of insulin-granule pH. Our results confirm the acidic nature of insulin granules under maintenance cell culture conditions, with an average luminal pH of ~5.8, and show that acidity is actively maintained, as evidenced by its near-neutralization upon treatment with the vacuolar H^+-ATPase inhibitor concanamycin. Additionally, by exploiting the intrinsic spatial resolution of FLIM, we highlight that granules which are proximal to the plasma membrane are slightly more acidic than those which are distal, a difference preserved even during the early phase of glucose-induced insulin secretion. This study lays the foundations for future investigations of granule pH in physiology and disease.

Insulin is synthesized in its immature form, pre-proinsulin, at the endoplasmic reticulum level[1]. After its conversion into proinsulin, it is transported to the trans-Golgi network (TGN) and then translocated into insulin secretory granules (ISG)[1]. At this level, the acidification of the luminal pH is supposed to be necessary for both the conversion of proinsulin into active insulin (with the release of the C-peptide fragment) and for the ISG maturation and secretion at the plasma membrane level[1,2]. Despite the crucial role played by pH regulation, a direct and accurate measurement of the absolute pH of ISGs in living cells is still missing.

The very first measurements of granule intraluminal pH performed almost 40 years ago, demonstrated that the pH of the ISG is in the 5.0–6.0 range and that maintaining the acidic condition is ATP-dependent. Yet these measurements referred to isolated granules, i.e. outside the realm of natural cellular environment[3,4]. The almost concomitant advent of pH-sensitive fluorescent probes paved the way for direct investigations of granule pH within living cells. In a seminal study, Pace and Sachs used the weak base Acridine Orange (AO) as pH probe[5]. They showed that β-cell granules in islet cultures could accumulate AO with a characteristic red shift, highlighting the presence of a pH gradient across the granule membrane (i.e. between granule lumen and cell cytoplasm)[5]. Unfortunately, due to the intrinsic photophysical characteristics of AO, it was not possible to provide a reliable estimate of the actual pH value of granules in cells. With similar limitations, in 2001 Barg and colleagues monitored granular pH by supplementing the extracellular solution with LysoSensor Green DND-189, a fluorescent probe, whose fluorescence intensity increases as pH decreases[6]. Although not quantitative in terms of absolute pH, the authors were able to confirm that granular acidification (driven by a V-type H+-ATPase in the granular membrane) is a decisive step in granule priming for exocytosis[6]. Following a similar approach, Stiernet and colleagues measured granule pH in islets but using Lysosensor DND-160, a variant allowing, in principle,

[1]NEST Laboratory - Scuola Normale Superiore, Pisa, Italy. [2]Fondazione Pisana per la Scienza ONLUS, Pisa, Italy. [3]NEST, Istituto Nanoscienze - CNR, Pisa, Italy. [4]Department of Surgical, Medical and Molecular Pathology, and Critical Care Medicine, University of Pisa, Pisa, Italy. [5]Present address: CNR IFC Istituto di Fisiologia Clinica, Pisa, Italy. ✉e-mail: valentina.delorenzi@sns.it; francesco.cardarelli@sns.it

ratiometric determination of absolute pH values in acidic compartments[7]. Yet, results were presented in terms of pH differences, rather than in terms of absolute pH. Still, the authors were able to show that an increase in glucose concentration induces a rapid and reversible decrease in granular pH in a metabolism and chloride-dependent manner[7]. By contrast, in a similar experiment using the fluorescent pH indicator Lysosensor Green DND-189, Eto and colleagues observed that, upon glucose stimulation, the pH of ISGs in pancreatic β-cells, was alkalinized by approximately 0.016 pH units[8].

At this stage, it is important to note that in the attempts reviewed so far, researchers employed dyes (such as acridine orange and Lysosensor variants) that are not specific to insulin granules but distributed across all acidic compartments of the cell, including endosomes and lysosomes, potentially affecting the final pH measurement. To bypass these limitations, Tompkins and colleagues, in 2002, targeted a genetically encoded pH sensor in the form of the pH-sensitive variant of green fluorescent protein (EGFP F64L/S65T) to insulin secretory vesicles in RIN1046-38 insulinoma cells by fusing the sensing moiety to the N-terminal leader sequence of human growth hormone[9]. The authors observed that glucose stimulation induces a decrease in granule pH, whereas inhibitors of the V-type H-ATPase increase pH and impair glucose effect[9]. Although specifically targeted to the insulin secretory pathway, this GFP-based pH sensor was intrinsically non-ratiometric, i.e. it reported only relative pH changes among different conditions. Worthy of mention, an attempt to overcome current limitations was performed by Neukman and coworkers by sending a quantitative pH reporter to the granule (i.e. eCFP fused to the ICA512-RESP18 homology domain in INS-1 cells) but has so far remained in the form of a preprint and has not yet undergone peer review[10].

To summarize, none of the reports available in the literature satisfy the two requirements of a reliable measurement of absolute pH in the ISG, i.e. (i) specific targeting of the pH reporter in the insulin secretory pathway and (ii) calibration of the reporter to obtain absolute pH values within the desired range. To tackle both issues simultaneously, we inserted the ratiometric and genetically encoded E^{1}GFP pH reporter within the C-peptide (C-pep) of proinsulin (see Fig. 2a). E^{1}GFP was selected as it is endowed with a pKa close to 6.0 and it demonstrated to be suitable for absolute pH measurements in acidic compartments[11]. Additionally, the insertion of E^{1}GFP into the C-pep was shown not to alter the sorting of the whole adduct into the ISG[12–14]. Phasor-based Fluorescence Lifetime Imaging Microscopy (FLIM) was used as a fast, robust, and fit-free method to measure ISG luminal pH independently of probe concentration, while also providing a spatial map of pH values.

Our results confirmed the acidic nature of insulin granules under maintenance cell-culturing conditions, with an average luminal pH of ~5.8, and showed that acidity is actively maintained, as evidenced by its near-neutralization upon treatment with the vacuolar H^+-ATPase inhibitor concanamycin. Additionally, by leveraging the intrinsic spatial resolution of FLIM, we highlighted that granules proximal to the plasma membrane are slightly more acidic with respect to distal ones, a difference preserved even during the early phase of glucose-induced secretion.

Results

Characterization of E^{1}GFP as a lifetime intracellular pH probe

To measure the pH in the lumen of ISGs, we utilized the E^{1}GFP pH probe. E^{1}GFP, part of the Y66-chrom protein family, contains a tyrosine residue at position 66, whose protonatable phenolic group makes the protein's optical properties sensitive to pH[15]. The nearby residue, i.e. E222, splits the protonated chromophore into the optically distinguishable states **A′** and **A** (Fig. S1a)[16]. Interestingly, it can be demonstrated that the overall set of three protonation equilibria mathematically behaves like a single-site deprotonation with a unique pK_a of 6.0[11,16]. At pH ≪ pK_a the absorption spectrum is dominated by the single band of **A′** state peaked around 410 nm (Fig. S1b). Conversely, at pH ≫ pK_a both the **A** and **B** states become predominant showing absorption bands at 402 nm and 509 nm, respectively (Fig. S1b)[11]. The protonation state of E222 significantly affects the emission properties of the **A′** and **A** states, by altering the excited state dynamics[17]. Although they can be excited at almost the same wavelength, the excited **A** state emits at 516 nm, while the excited **A′** state emits at 507 nm (Fig. S1b)[11]. This spectral difference underlies the reported intracellular ratiometric pH sensing capability of E^{1}GFP[11]. FLIM provides a valuable alternative to ratiometric sensing, being free of artifacts due to wavelength-dependent scattering and without the intrinsic loss of S/N due to the computed ratio between optical signals[18]. The pH sensor E^{2}GFP, which differs from E^{1}GFP only by the S65T substitution, has been successfully applied to intracellular pH measurements by FLIM using the phasor approach[19], but displays a pK_a equal to 7 which is not suitable for the measurements of acidic organelles, i.e. ISGs. To test whether the fluorescence lifetime properties of E^{1}GFP could be reliably used for intracellular pH measurements using FLIM, we expressed and purified recombinant His-tagged E^{1}GFP (Fig. S2) and measured the fluorescence lifetime in solutions buffered at pH 4.85 and pH 8.0, to obtain almost pure **A′** and **A** forms, respectively. We found that the excited **A** state emits a mono-exponential decay characterized by $\tau = 3.5$ ns (Fig. 1a). In contrast, the excited **A′** state exhibits biexponential decay characterized by an average lifetime of $\langle\tau\rangle = 0.83$ ns (Fig. 1a). We subsequently performed FLIM measurements on the purified protein diluted in solutions buffered at various pH values (Fig. 1b, c). Lifetime data were analyzed using the phasor approach. Technically, for each pixel in the image, the fluorescence decay measured in the time domain was mapped onto the so-called "phasor" plot, where a phasor has two coordinates: the real and imaginary parts of the Fourier transform of the fluorescence lifetime decay, calculated at the angular repetition frequency of the laser in the measurement. The calculated phasors (one for each pixel) fall within the half-disk centered at (½,0) with radius ½ and positive *x*, where the zero lifetime is located at (1,0) and the infinite lifetime at (0,0). This suggests that by taking the Fourier transformation of a measured decay curve, the lifetime can be estimated based on the position of the phasor in the reference system of the universal (semi)circle. The distribution of phasor points originating from FLIM measurements appears on the universal circle for mono-exponential decays, or inside the circle for multi-exponential decays. In this work, phasor analysis was carried out using a cloud-based custom Python routine that we previously published[20]: the decays measured pixel-by-pixel in the image originate from a phasor cluster whose position depends on the average fluorescence lifetime (Fig S3a). The average lifetime was calculated by determining the phasor barycenter (Fig. S3b). As expected for a single-site protonation behavior, the phasor analysis of the pH calibration revealed a linear distribution of the phasor barycenters ($R^2 = 0.9873$). We found that the barycenter for the highest pH was located near the universal circle, indicating a nearly mono-exponential decay at high pH, in agreement with the predominant excitation of the **A** state (Fig. 1c). At the lowest pH tested, the phasor fell inside the universal circle, witnessing the multi-exponential nature of the decay with a phasor-calculated lifetime close to 1.0 ns, in keeping with the in vitro measurements of **A′** state emission (Fig. 1c).

C-pep-E1GFP sensor calibration in INS-1E cells

To target the E^{1}GFP pH reporter to the ISGs, we generated the C-pep-E^{1}GFP construct in which the E^{1}GFP coding sequence is inserted within the C-pep of proinsulin (Fig. 2a) by site-directed mutagenesis of the previously described C-pep-EGFP plasmid[13]. To check for proper localization at the granular level, INS-1E cells were transiently transfected with C-pep-E^{1}GFP plasmid and stained with a granule-specific Zn^{2+} indicator namely ZIGIR[21]. The E^{1}GFP signal was enriched in dot-like structures, located both in the cytoplasm and at the plasma membrane level, and showed a good co-localization with ZIGIR (Pearson coeff. = 0.53, M1 = 0,7142, M2 = 0,3466; $n = 15$ cells) confirming the targeting to the ISGs (Fig. 2b). The relatively low value of Mander's coefficient M2 might be attributed to the presence of the genetically encoded protein in the biogenesis structures of the granule and in not fully mature ISGs, which are not stained by ZIGIR. Additional co-localization experiments were carried out as a means of excluding that the cytoplasmic granules could be degradative organelles (Fig. S4). C-pep-EGFP expressing INS-1E cells were treated with LysoTracker to stain for lysosomes or co-transfected with mRFP-LC3b for autophagosome labeling. Phogrin-mCherry co-transfection served as a positive control for ISG

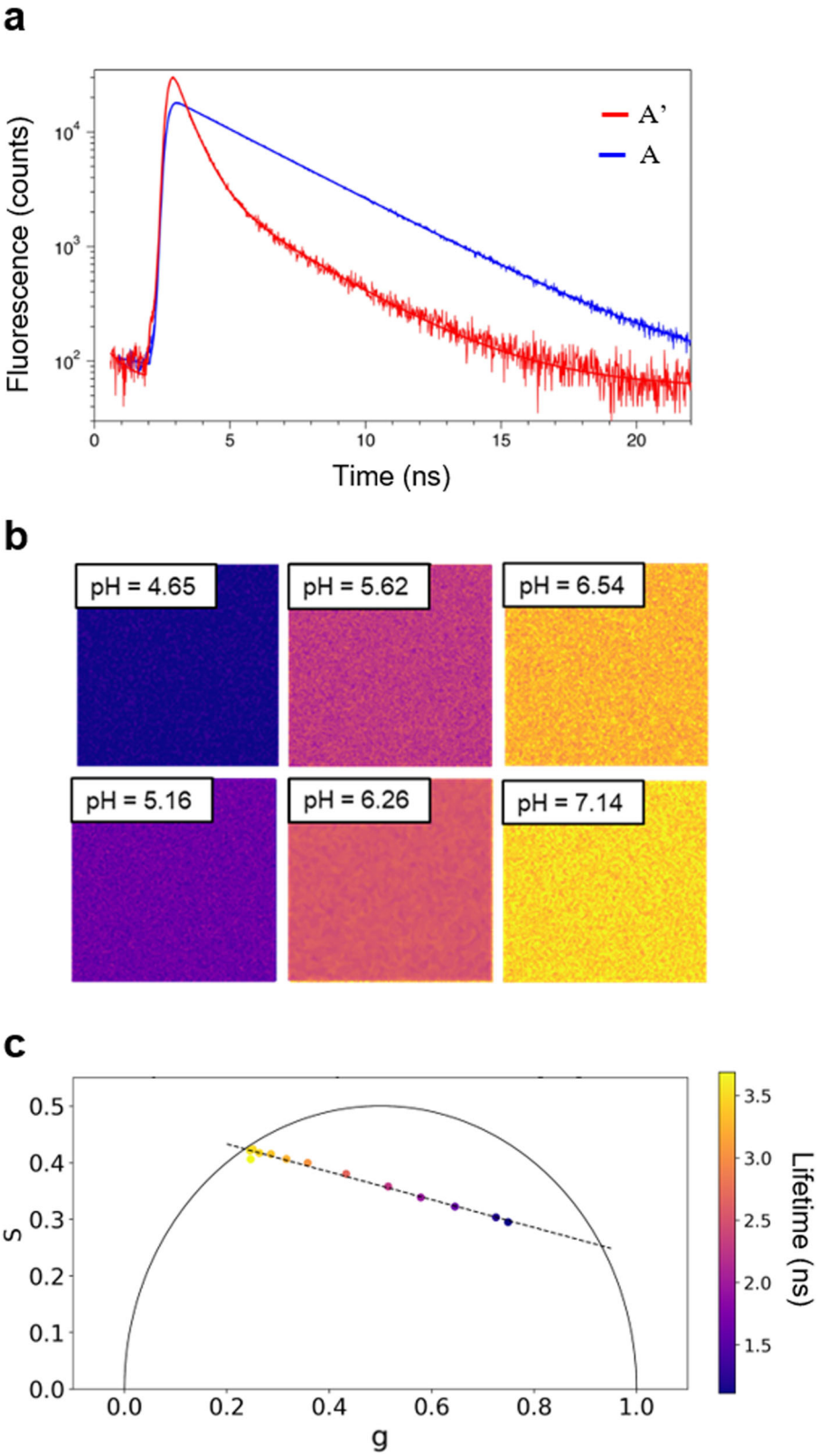

Fig. 1 | E^{1}GFP in vitro calibration. a Lifetime decays of A′ (red) and A (blue) upon excitation at 405 nm and collection in the 480–550 nm range. Purified recombinant E^{1}GFP was incubated in citrate/phosphate buffer at pH 4.85 or 8.0 to obtain almost pure A′ and A forms, respectively. **b** Representative FLIM images of recombinant E^{1}GFP diluted in calibration buffer with the indicated pH. Images are pseudo-colored based on the lifetime calculated per pixel according to the color bar depicted in the figure. **c** Phasor plot analysis of the images of panel **b**. Phasor barycenters with SD and the corresponding linear regression fit are reported.

targeting. Pearson's coefficients calculated from 2-channel images (Fig. S4b) confirmed a strong co-localization between the C-pep reporter and ISGs (Pearson coeff. = 0.77), in contrast to low co-localization with autophagosomes (Pearson coeff. = 0.11) and lysosomes (Pearson coeff. = 0.28). To calibrate the probe in the cellular environment, INS-1E cells expressing C-pep-E^{1}GFP were permeabilized with nigericin, incubated in buffers with known pH values, and analyzed using FLIM (Fig. 2c). As for the recombinant protein, phasors were linearly distributed along a segment within the universal circle (R^2 = 0.997) (Fig. 2d). The fluorescence lifetime as a function of pH was satisfactorily fitted to a single-site sigmoidal model (R^2 = 0.9985) yielding a pKa of 5.91, this value is very close to the pKa previously measured using fluorescence intensity-based ratiometric imaging[11] (Fig. 2e). This strongly suggests the existence of the same **A′/A** equilibrium observed in vitro also when E^{1}GFP is inserted within the C-pep

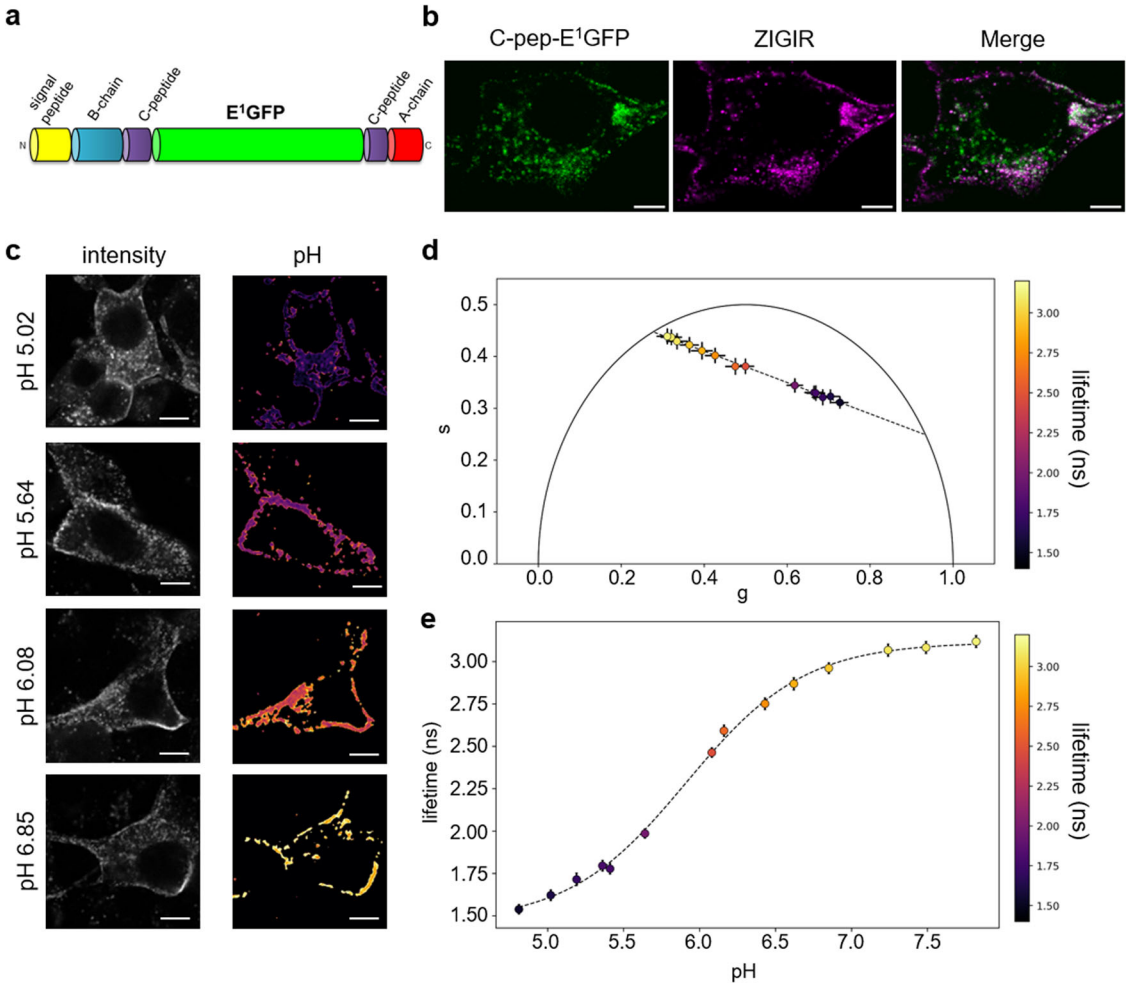

Fig. 2 | Calibration of the C-pep-E^{1}GFP sensor in INS-1E cells. a Schematic representation of the pH sensor. The cartoon shows the pre-proinsulin protein domains highlighting the E^{1}GFP insertion within the C-pep. **b** Representative confocal images of C-pep-E^{1}GFP transfected INS-1E cells. Co-localization between C-pep-E^{1}GFP (green) and ZIGIR as insulin granules dye (magenta) is highlighted in the merge panel (white). Scale bar: 5 µm. **c** Calibration of the sensor in living cells. Representative images of C-pep-E^{1}GFP transfected INS-1E cells incubated with buffers of the indicated pH and permeabilized with 10 µM nigericin. Intensity images are shown alongside pseudo-colored images based on fluorescence lifetime calibration, using the LUT reported in the figure. Scale bar: 10 µm. **d** Phasor plot analysis of the cell calibration corresponding to (**c**). Phasor barycenters with SD at different pH and the linear fitting through the experimental points are depicted. **e** The resulting calibration curve showing the correlation between pH and lifetime. Average lifetime ± SD is shown. Non-linear fitting was performed using the log(agonist) vs. response - Variable slope (four parameters) equation. The strict adherence of the plot to a single-site titration curve suggests that the A′/A equilibrium of E^{1}GFP is into play also when the protein is expressed intracellularly.

and expressed in cells, a crucial property for the ability of the probe to report on intracellular pH. Worthy of note, the absolute values of the fluorescence lifetimes measured in living cells were lower than those obtained in bulk solutions, an effect that might be attributed to the different microenvironment or to crowding effects within the ISGs, both leading to the increase of the non-radiative rate from the excited state. Nonetheless, the high adherence of the intracellular titration plot to the in vitro single-site binding curve suggests that the lifetime reduction effects have a moderate to negligible pH dependence, and they posit the different environmental properties of the intracellular milieu as compared to the buffer solutions as a more convincing explanation of this photophysical phenotype.

Measurement of ISGs pH in standard culturing conditions

After calibration, the C-pep-E^{1}GFP sensor was employed to measure the luminal pH of ISGs in INS-1E cells under standard culturing conditions (see "Methods" section for medium supplementation details) (Fig. 3a). By calculating the phasor barycenter, an average pH of 5.78 ± 0.06 was determined for the ISGs, a value in keeping with previous indications of the slight acidity of the granular pH (see "Introduction" section). It is worth mentioning that FLIM acquisitions require signal integration over time in order to collect sufficient photons for phasor analysis. Consequently, the apparent size and/or shape of dynamic dot-like structures (e.g. ISGs) within cells may be altered. Fig. S5 presents a representative example where the degree of signal integration is mirrored by the enlargement and deformation of the labeled ISGs located in the cytoplasm. If, instead of computing the barycenter (i.e. to determine average pH), the cluster lifetime distribution is described in its entirety using a lifetime-dependent LUT, different regions of the cell with varying lifetimes can be highlighted. We observed a slight, yet significant, difference in average pH between granules located in proximity to the plasma membrane (5.72 ± 0.06) and granules within the cytoplasm (5.83 ± 0.09) (Fig. 3b). More in detail when examining individual cells, heterogeneity is observed: some cells show almost no difference, while others exhibit differences of up to approximately 0.3 pH units. This differing behavior may arise from genuine heterogeneity within the cell population or could be attributed to technical aspects of the measurements, such as the lowest resolution along the z-axis. This could result in plasma membrane granules being inadvertently included within the designated cytoplasmic ROI, thereby reducing the observed pH difference. Overall, the difference in pH between granules at the membrane level and granules in the cytoplasm aligns with what is thought to happen during granule biogenesis and

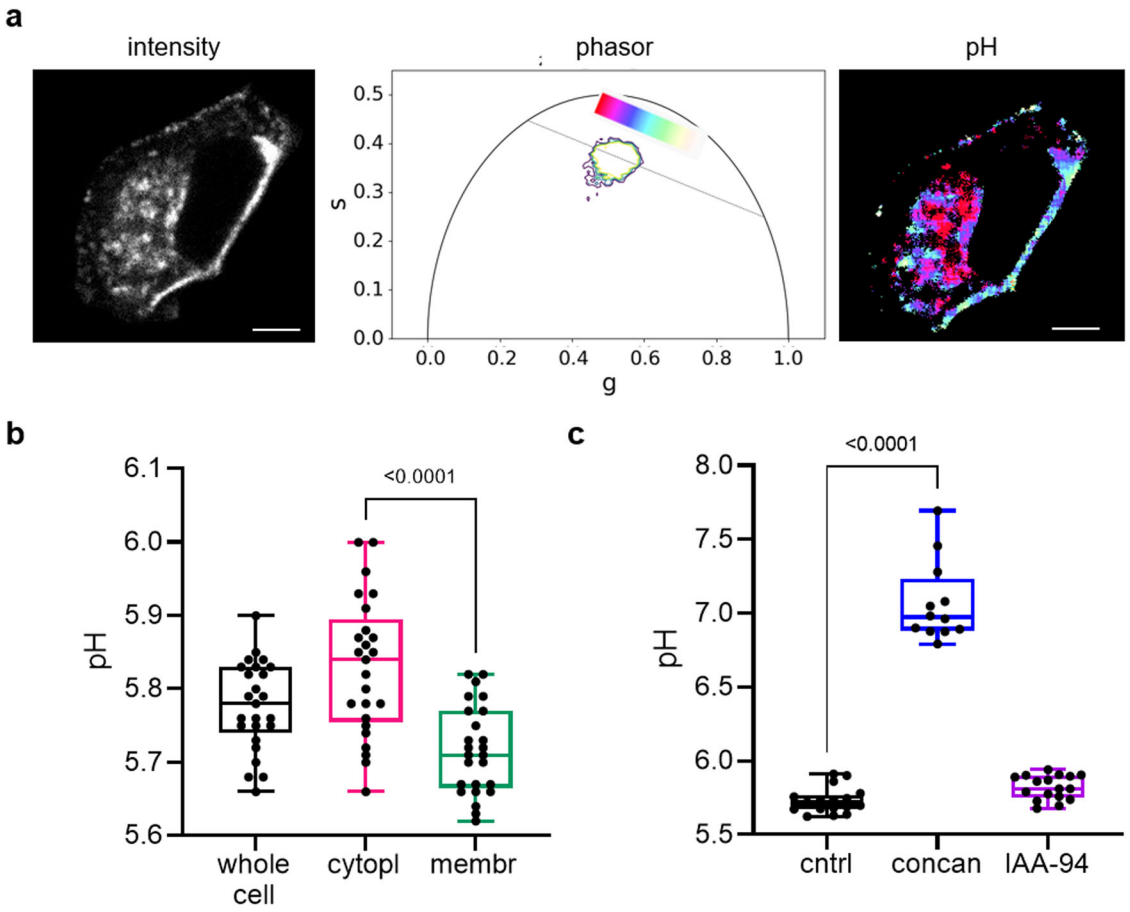

Fig. 3 | Measurement of ISG pH in INS-1E cells. a Representative image of INS-1E cell transfected with C-pep-E^{1}GFP. Cells were imaged 48 h post-transfection in a standard growth medium. Panels display the intensity, phasor plot, and calculated pH of the fluorescence signal of a representative cell. Scale bar: 2 µm. **b** Box plot (min to max) of the calculated average ISG pH in three regions of interest i.e. the whole cell, cytoplasm, and plasma membrane. $n = 25$ cells from 4 independent experiments. **c** C-pep-E^{1}GFP transfected INS-1E cells were treated with 100 nM concanamycin or 100 µM R(+)-IAA-94 for 1 h at 37 °C and imaged by FLIM. Box plot (min to max) of concanamycin ($n = 12$) and IAA-94 ($n = 17$) treated cells compared to control cells ($n = 17$) from 3 independent experiments.

trafficking from the TGN to the plasma membrane[1]. This process involves a series of maturation steps, during which acidification and removal of coat proteins coincide with the conversion of proinsulin to insulin[3,22,23]. It is worth noting that in this process a key role has been ascribed to the vesicular ATP-dependent proton pump (V-ATPase), which increases the activity of the proinsulin-converting enzymes PC1/3 and PC2[3,24,25]. Acidification begins shortly after budding from the TGN and progresses over approximately 30 min, during this time proinsulin is converted to insulin and the protein coat is lost. The role of V-ATPase was confirmed here by probing granule pH in INS-1E cells in the presence of the vacuolar H+-ATPase inhibitor concanamycin. As expected, concanamycin induced a fast and robust pH shift towards neutrality (pH = 7.07 ± 0.27). Interestingly, by contrast, granule pH was not significantly affected by inhibition of chloride channels using the channel blocker R(+)-IAA-94 (pH = 5.82 ± 0.08 in the presence of the drug, as compared to pH = 5.74 ± 0.09 under control conditions). This suggests that other counterions and/or chloride channels insensitive to IAA-94 may contribute to granule pH regulation (Fig. 3c). This lack of effect has been previously reported[10]. Further experimentation, possibly involving a chloride sensor, is needed to clarify this point.

Monitoring ISGs pH upon glucose stimulation

It should be noted that glucose stimulation is another granular pH regulator that is variably evoked in the literature, although with contrasting claims. While two independent studies suggest that glucose stimulation induces acidification of the ISG lumen[7,9], Eto and coworkers reported that the same stimulus results in acute alkalinization of granule lumen[8]. To probe the glucose-stimulation effect on granule pH, C-pep-E^{1}GFP transfected INS-1E cells were first incubated at low glucose concentration for 45 min (i.e. SAB buffer supplemented with 2.2 mM glucose) and then switched to high glucose concentration, by glucose addition to a final concentration of 16.7 mM. FLIM was performed right before glucose addition (0 min) and 5 and 10 min after stimulation (Fig. 4). Not surprisingly, visual inspection of the intensity images collected at different times of exposure to glucose suggests that a fraction of granules is lost due to secretion (Fig. 4a). Despite this, the color-coded map of the cell shows that a difference in lifetime between granules in proximity of the plasma membrane and granules in the cytoplasm persists throughout the first phase of the secretion process (Fig. 4b). This is more quantitatively expressed by lifetime data extracted from single-cell segmentation of $n = 11$ stimulated cells (Fig. 4c). By comparing the granule pH over time, a slight trend toward higher pH is observed, particularly in membrane granules, but it did not reach statistical significance. Of note, the pH of membrane granules of cells incubated with SAB buffer 2.2 mM glucose (5.47 ± 0.17, 0 min condition of Fig. 4c) was significantly lower compared to membrane granule of cells maintained in standard culture condition (5.72 ± 0.06, Fig. 3b). To determine whether the pH difference arises from serum starvation or reduced glucose concentration, we compared maintenance conditions (i.e. the complete medium contains 11 mM glucose) with SAB buffer supplemented either with 2.2 mM or with 11 mM glucose (Fig. S6). Remarkably, the pH of membrane-associated ISGs also decreased in SAB with 11 mM glucose, suggesting that the observed reduction in pH is likely due to the use of a serum-free buffer rather than reduced glucose concentration.

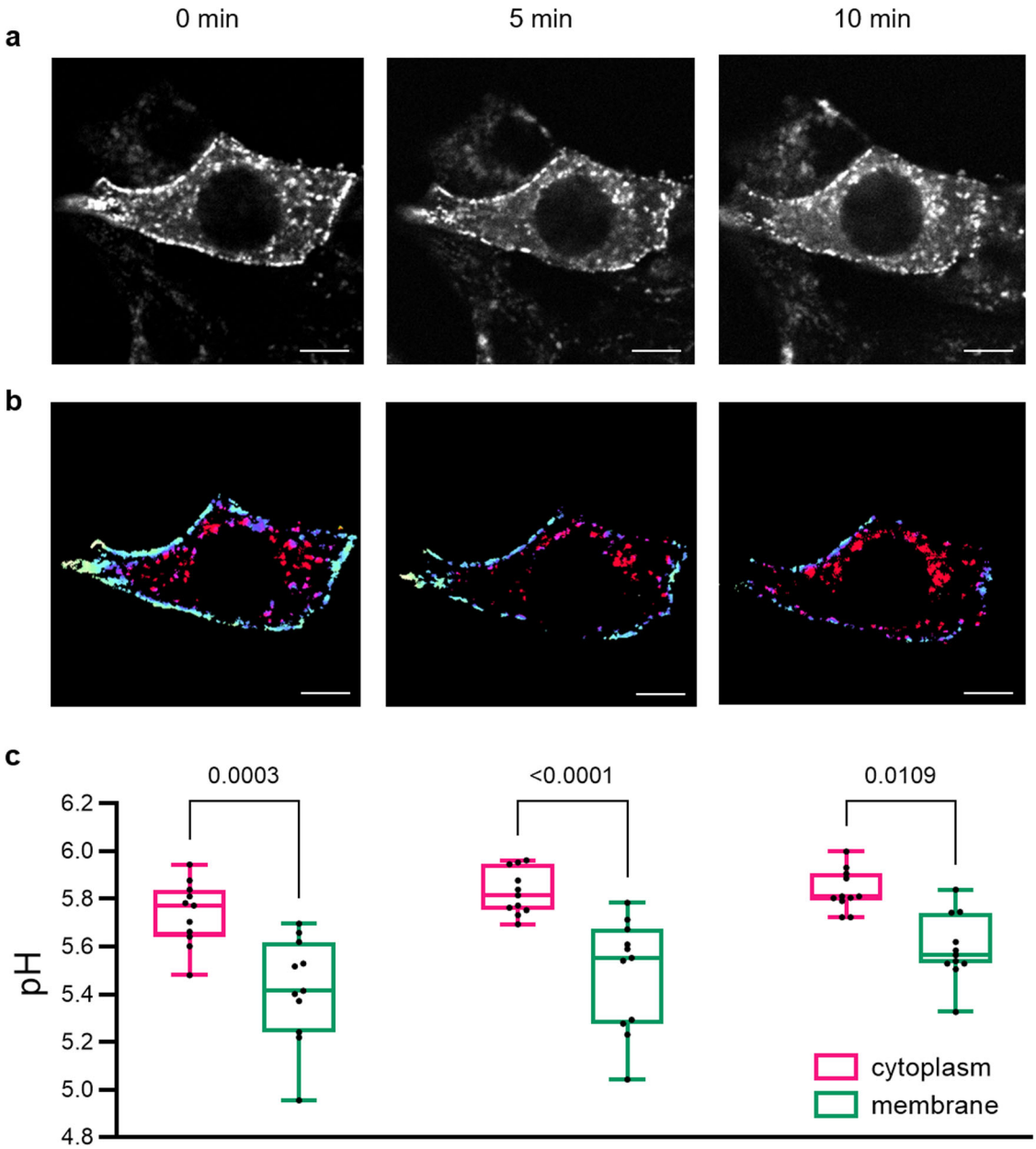

Fig. 4 | ISG pH measurements during glucose stimulation. a, **b** C-pep-E^{1}GFP transfected INS-1E cells were stimulated with glucose following the protocol described in the "Methods" section. Intensity images (**a**) and pH pseudo-colored images (**b**) of a representative cell at three different time-points are shown. Scale bar: 10 µm. **c** Box plot (min to max) derived from (**a**, **b**) showing the comparison between the pH of granules located in the cytoplasm (magenta) versus granules close to the plasma membrane (green) before (0 min) and after glucose stimulation (5 min and 10 min), $n = 11$ from 3 independent experiments.

Discussion

As already pointed out in the "Introduction" section of this work, no report thus far satisfactorily addressed the two requirements for a reliable measurement of the absolute pH in the ISG, i.e. (i) specific targeting of the pH reporter in the granule and (ii) calibration of the reporter to obtain affordable absolute pH values. Here we tackled these issues simultaneously by inserting the genetically encoded E^{1}GFP pH reporter (endowed with a pKa close to 6.0) within the C-pep of proinsulin, exploited as a specific marker of the ISG. From a methodological perspective, a few aspects are worth mentioning. First, the choice of a pH-sensitive mutant of the GFP family constitutes an attractive and flexible strategy as these indicators, contrary for instance to fluorogenic organic dyes, can be expressed in cells, tissues, and whole organisms as fusion chimeras with specific targeting motifs to monitor pH or other parameters[18,26] in specific subcellular compartments with minimal associated (photo)toxicity. Second, FLIM provides an excellent concentration-independent and single-excitation wavelength/emission interval alternative to classical ratiometric measurements, which instead are typically accompanied by a reduction of the signal-to-noise ratio at low intensities and by intrinsic error amplification of the ratio operation. Lastly, although this is not the first application of FLIM on pH-sensitive fluorescent proteins for intracellular measurements[27,28], its combination with the phasor transformation of lifetime data is promoted here as a fast, robust, and fit-free approach to measure the pH in secretory vesicles while also providing a spatial map of the measured parameters, along the lines of previous work on this subject conducted by some of us[19]. From a biological perspective, the results obtained here confirm the slightly acidic nature of insulin granules under maintenance cell-culturing conditions, with an average luminal pH of about 5.8, and showed that acidity is actively maintained. In addition, thanks to the intrinsic spatial resolution of FLIM, it is highlighted that granules proximal to the plasma membrane are slightly

more acidic with respect to distal ones, a difference preserved even during the early phase of glucose-induced secretion. Speculatively, it might be assumed that the maintenance of a pH difference between membrane and cytoplasm during the secretory process - i.e. in the presence of a loss of membrane granules due to secretion and of a concomitant arrival of new granules from the cytoplasm - supports the idea that the priming of new granules from the cytoplasm to the membrane under glucose stimulation is accompanied by their acidification. This, in turn, would agree with at least one of the prevailing views that can be found in the literature[6,7,9]. A definitive demonstration that granule acidification occurs during its mobilization to the membrane would involve combining pH measurements at the single-granule level with high time-resolution localization of the individual granules to simultaneously track the granule and its pH in the intracellular reference system. This measurement, technically possible using E^{1}GFP as a ratiometric emission sensor whose split signal in two channels is used for both pH calculation and localization/tracking, would in turn entail, as mentioned above, optimization of the imaging conditions to maximize signal-to-noise ratio and minimize the intrinsic error amplification associated with the ratio operation.

In conclusion, this report paves the way for using phasor-FLIM combined with calibrated genetically encoded reporters to monitor granule pH at the temporal (seconds-to-minutes) and spatial (subcellular) resolution of interest for investigating insulin secretion in physiology and disease.

Methods

Plasmids construction

E^{1}GFP protein harbors two mutations (T65S and T203Y) compared to EGFP[11]. Therefore, to generate the C-pep-E^{1}GFP construct, C-pep-EGFP plasmid[13] was subjected to two rounds of site-directed mutagenesis using QuikChange XL Site-Directed Mutagenesis Kit (Agilent Technologies). The forward sequence for the T65S mutation was 5′-CCCACCCTCGTGACC ACCCTGAGCTACGGCGTGCAGTGCTTC-3′, for the T203Y 5′-CAACC ACTACCTGAGCTACCAGTCCGCCCTGAG-3′. For the bacterial expression of recombinant His-tagged E^{1}GFP, the E^{1}GFP sequence was amplified from C-pep-E^{1}GFP construct by PCR and cloned NdeI/BamHI in pET28c+ to generate pET-His-E^{1}GFP plasmid. pmRFP-LC3b was a gift from Tamotsu Yoshimori (Addgene plasmid # 21075; http://n2t.net/addgene:21075; RRID: Addgene_21075[29]). The Phogrin-mCherry construct has already been described previously[12].

Expression and purification of recombinant E^{1}GFP

pET-His-E1GFP construct was transformed in BL21 (DE3) competent cells (Invitrogen). Cells were grown at 37 °C till OD600 of about 0.6, and protein expression was induced by the addition of 250 µM IPTG for 24 h at 28 °C. Cells were harvested by centrifugation and frozen at −20 °C. Cell pellet was resuspended in ice-cold lysis buffer (40 mM Tris-HCl pH 8.0, 300 mM NaCl, 1 mM MgCl2 supplemented with EDTA-free protease inhibitor cocktail (Roche) and DNAseI) and lysed by sonication on ice followed by 1 h treatment with 1% Triton-X100 at 4 °C. The bacterial lysate was cleared by centrifugation and filtered through a 0.2 µm filter before loading onto a Bio-Scale Mini Profinity IMAC Cartridge (Bio-rad#7324614) in a fast protein liquid chromatography system (AKTAxpress, GE Healthcare). The His-tagged protein was eluted using a 0–500 mM imidazole gradient. Imidazole was then removed by buffer exchange in 20 mM diethanolamine pH = 8.5. Protein purity was evaluated by SDS-PAGE (Fig. S2a), and the concentration was determined by UV absorption measurements using the extinction coefficient calculated in ref. 16. The absorption spectrum (Fig. S2b) was recorded at RT on a Jasco V550 spectrophotometer (JASCO, Easton, MD, USA) with the following collection parameters: bandwidth 2 nm, scanning speed 1000 nm/min, and data resolution 1 nm.

Cell culture, transfection, and treatments

INS-1E cells[30] (kindly provided by Prof. C. Wollheim, University of Geneva, Medical Center) were cultured in RPMI 1640 medium containing 11 mM glucose and supplemented with 10% heat-inactivated fetal bovine serum, 100 Units/ml penicillin, 100 µg/ml streptomycin, 2 mM glutamine, 10 mM HEPES, 1 mM sodium pyruvate, and 50 µM β-mercaptoethanol at 37 °C in a humidified 5% CO_2 atmosphere. Cells have been tested for mycoplasma contamination and found negative. For live cell imaging, INS-1E cells were plated onto IbiTreat µ-Dish 35 mm (Ibidi cat #81156) and transfected the day after using Lipofectamine 2000 (Life Technologies), following the manufacturer's instructions. Cells were imaged 48 h post-transfection. Drugs were supplemented to the standard culture medium as follows: concanamycin (MedChemExpress HY-N1724) was used at 100 nM for 1 h at 37 °C and R(+)-IAA-94 (MedChemExpress HY-12693) at 100 µM for 1 h at 37 °C. For glucose stimulation, C-pep-E^{1}GFP transfected INS-1E cells were incubated for 45 min in SAB buffer (114 mM NaCl, 4.7 mM KCl, 1.2 mM KH_2PO_4, 2.5 mM CaCl2, 1.16 mM MgSO4, and 20 mM HEPES (pH 7.4)) containing 2.2 mM glucose prior to microscope acquisitions, then glucose was added to reach a final concentration of 16.7 mM.

pH sensor calibration in vitro and in living cells

Titration of E^{1}GFP lifetime versus pH was performed by diluting recombinant E^{1}GFP to a final concentration of 2.1 µM in a citrate (2 mM)/phosphate (10 mM) buffer adjusted to the desired pH by addition of 1 M NaOH. WillCo-dish® Glass Bottom Dishes (WillCo Wells, cat #HBST-3522) were incubated with 2% BSA for about 40 min at 37 °C to avoid protein sticking to the dish surface. For sensor calibration in living cells, C-pep-E^{1}GFP transfected INS-1E cells were incubated for 10 min with an enriched K^+ buffer containing 120 mM potassium gluconate, 40 mM sodium gluconate, 20 mM HEPES, 0.5 mM $CaCl_2$, 0.5 mM $MgSO_4$ adjusted to the desired pH with NaOH and supplemented with 10 µM nigericin. The final pH value used for the calibration curve was measured right after the FLIM acquisition.

Spectroscopic and lifetime measurements of pure low-pH and high-pH states in vitro

Absorption spectroscopy of purified recombinant E^{1}GFP was carried out according to the procedure reported in ref. 16. Almost pure **A′** and **A** forms (see text for details) were addressed by setting the pH to 4.85 or 8, respectively by a citrate (2 mM)/phosphate (10 mM) buffer adjusted to the desired pH by addition of 1 M NaOH. Emission spectra were obtained by exciting the protein at 405 nm and collecting emission in the 450–650 nm range with a 5 nm step. Lifetime decays of the protein were obtained by exciting at 405 nm and collecting emission in the 480–550 nm range. In both cases, measurements were carried out in a Leica TCS SP5 SMD inverted confocal microscope (Leica Microsystems AG, Buffalo Grove, IL) equipped with an external pulsed diode laser for excitation at 405 and 470 nm and a time-correlated single photon-counting acquisition card (PicoHarp 300; PicoQuant, Berlin, Germany) connected to internal spectral detectors. The laser repetition rate was set to 40 Hz. Acquisitions lasted until 100–200 photons per pixel were collected, at a photon-counting rate of 100–500 kHz.

Two-photon microscopy, phasor-FLIM measurements, and data analysis

Phasor-FLIM measurements were carried out on an Olympus FVMPE-RS microscope coupled with a two-photon Ti:sapphire laser with an 80-MHz repetition rate (MaiTai HP, SpectraPhysics) and FLIMbox system for lifetime acquisition (ISS, Urbana Champaign). Measurements were performed at 37 °C in a humidified 5% CO_2 atmosphere. E^{1}GFP was excited at 800 nm and the emission was collected by using a 30× planApo silicon immersion objective (NA = 1.0) in the 500–540 nm range. Calibration of the ISS Flimbox system was performed by measuring the known mono-exponential lifetime decay of Fluorescein at pH = 11.0 (i.e. 4.0 ns upon excitation at 800 nm, collection range: 500–540 nm). To prepare the calibration sample, 100 mM Fluorescein solution in EtOH was diluted 1:5000 in 0.1 M NaOH at pH 11.0. For each measurement, a 512 × 512 pixels image of FLIM data was collected until about 100k counts in the brightest pixel were achieved. The phasor analysis of experimental lifetime acquisitions was performed by using custom dedicated routines implemented in Python 3.6 as described in ref. 20.

Co-localization analysis

INS-1E cells were plated on IbiTreat µ-Dish 35 mm and transfected with C-pep-E^{1}GFP plasmid or co-transfected with C-pep-EGFP plasmid and pmRFP-LC3b or Phogrin-mCherry plasmid as described above. 48 h post-transfection, cells were incubated with 0.2 µM ZIGIR for 15 min or LysoTracker Deep Red (Thermo Fisher, cat#L12492) diluted 1:50,000 for 30 min and imaged on an inverted Zeiss LSM 800 confocal microscope (Jena, 439 Germany) or on an Olympus FV3000 confocal microscope. The acquisition was performed using a 63×/NA 1.4 oil-immersion objective, setting the pinhole aperture at 1 Airy. 2-channels images acquired in sequential mode to avoid spectral cross-talk were used to calculate Pearson's correlation coefficient. Fluorescence signals were collected as follows: E^{1}GFP was excited with a 405 laser and emission was collected between 400 and 550 nm. EGFP was excited at 488 nm and collected between 500 and 600 nm. mCherry and mRFP were excited with a 561 nm laser with emission collected between 570 and 670 nm. ZIGIR was excited with a 561 nm laser and detected in the 550–700 nm window. Lastly, LysoTracker Deep Red was excited at 631 nm and collected between 650 and 750 nm. Pearson's correlation coefficient was calculated using the JaCoP plugin for ImageJ software.

Statistics and reproducibility

After checking the normality with the Shapiro–Wilk test, the statistical significance was evaluated by a one-way ANOVA test with multiple comparisons. *P* values are reported in figures as exact values. All experiments were repeated at least three times and reproducibility was confirmed.

Reporting summary

Further information on research design is available in the Nature Portfolio Reporting Summary linked to this article.

Data availability

All data supporting the findings of this study are available within the paper, the Supplementary Information, and the Supplementary Data. The newly generated plasmids described above have been deposited in the Addgene repository (Addgene ID#233884 for pCpep-E^{1}GFP and ID#233885 for pET-His-E^{1}GFP).

Received: 24 August 2024; Accepted: 17 February 2025;
Published online: 25 February 2025

References

1. Omar-Hmeadi, M. & Idevall-Hagren, O. Insulin granule biogenesis and exocytosis. *Cell. Mol. Life Sci.* https://doi.org/10.1007/s00018-020-03688-4 (2021).
2. Germanos, M., Gao, A., Taper, M., Yau, B. & Kebede, M. A. Inside the insulin secretory granule. *Metabolites* https://doi.org/10.3390/metabo11080515 (2021).
3. Orci, L. et al. Conversion of proinsulin to insulin occurs coordinately with acidification of maturing secretory vesicles. *J. Cell Biol.* **103**, 2273–2281 (1986).
4. Hutton, J. C. The internal pH and membrane potential of the insulin-secretory granule. *Biochemical. J.* **204**, 171–178 (1982).
5. Pace, C. S. & Sachs, G. Glucose-induced proton uptake in secretory granules of β-cells in monolayer culture. *Am. J. Physiol. Cell Physiol.* **242**, C382–C387 (1982).
6. Barg, S. et al. Priming of insulin granules for exocytosis by granular Cl-uptake and acidification. *J. Cell Sci.* **114**, 2145–2154 (2001).
7. Stiernet, P., Guiot, Y., Gilon, P. & Henquin, J. C. Glucose acutely decreases pH of secretory granules in mouse pancreatic islets: mechanisms and influence on insulin secretion. *J. Biol. Chem.* **281**, 22142–22151 (2006).
8. Eto, K. et al. Glucose metabolism and glutamate analog acutely alkalinize pH of insulin secretory vesicles of pancreatic β-cells. *Am. J. Physiol. Endocrinol. Metab.* **285**, E262–E271 (2003).
9. Tompkins, L. S., Nullmeyer, K. D., Murphy, S. M., Weber, C. S. & Lynch, R. M. Regulation of secretory granule pH in insulin-secreting cells. *Am. J. Physiol. Cell Physiol.* **283**, C429–C437 (2002).
10. Neukam, M., Sönmez, A. & Solimena, M. FLIM-based pH measurements reveal incretin-induced rejuvenation of aged insulin secretory granules. Preprint at *bioRxiv* https://doi.org/10.1101/174391 (2017).
11. Serresi, M., Bizzarri, R., Cardarelli, F. & Beltram, F. Real-time measurement of endosomal acidification by a novel genetically encoded biosensor. *Anal. Bioanal. Chem.* **393**, 1123–1133 (2009).
12. Ferri, G. et al. Insulin secretory granules labelled with phogrin-fluorescent proteins show alterations in size, mobility and responsiveness to glucose stimulation in living β-cells. *Sci. Rep.* **9**, 2890 (2019).
13. Rizzo, M. A., Magnuson, M. A., Drain, P. F. & Piston, D. W. A functional link between glucokinase binding to insulin granules and conformational alterations in response to glucose and insulin. *J. Biol. Chem.* **277**, 34168–4175 (2002).
14. Watkins, S. et al. Imaging secretory vesicles by fluorescent protein insertion in propeptide rather than mature secreted peptide. *Traffic* **3**, 461–471 (2002).
15. Nifosì, R., Storti, B. & Bizzarri, R. Reversibly switchable fluorescent proteins: "the fair switch project. *Riv. Nuovo Cim.* **47**, 91–178 (2024).
16. Bizzarri, R. et al. Green fluorescent protein ground states: the influence of a second protonation site near the chromophore. *Biochemistry* **46**, 5494–5504 (2007).
17. Chattoraj, M., King, B. A., Bublitz, G. U. & Boxer, S. G. Ultra-fast excited state dynamics in green fluorescent protein: Multiple states and proton transfer. *Proc. Natl Acad. Sci. USA* **93**, 8362–8367 (1996).
18. Battisti, A. et al. Imaging intracellular viscosity by a new molecular rotor suitable for phasor analysis of fluorescence lifetime optical nanosensing in cells. *Anal. Bioanal. Chem.* **405**, 6223–6233 (2013).
19. Battisti, A. et al. Intracellular pH measurements made simple by fluorescent protein probes and the phasor approach to fluorescence lifetime imaging. *Chem. Commun.* **48**, 5127–5129 (2012).
20. Bernardi, M. & Cardarelli, F. Phasor identifier: a cloud-based analysis of phasor-FLIM data on Python notebooks. *Biophys. Rep.* **3**, 100135 (2023).
21. Ghazvini Zadeh, E. H. et al. ZIGIR, a granule-specific Zn2+ indicator, reveals human islet α cell heterogeneity. *Cell Rep.* **32**, 107904 (2020).
22. Orci, L. et al. Direct identification of prohormone conversion site in insulin-secreting cells. *Cell* **42**, 671–681 (1985).
23. Orci, L. et al. Proteolytic maturation of insulin is a post-Golgi event which occurs in acidifying clathrin-coated secretory vesicles. *Cell* **49**, 865–868 (1987).
24. Rhodes, C. J., Lucas, C. A., Mutkoski, R. L., Orci, L. & Halban, P. A. Stimulation by ATP of proinsulin to insulin conversion in isolated rat pancreatic islet secretory granules. Association with the ATP-dependent proton pump. *J. Biol. Chem.* **262**, 10712–10717 (1987).
25. Davidson, H. W., Rhodes, C. J. & Hutton, J. C. Intraorganellar calcium and pH control proinsulin cleavage in the pancreatic β cell via two distinct site-specific endopeptidases. *Nature* **333**, 93–96 (1988).
26. Storti, B. et al. An efficient Aequorea victoria green fluorescent protein for stimulated emission depletion super-resolution microscopy. *Int. J. Mol. Sci.* **23**, 2482 (2022).
27. Poëa-Guyon, S., Pasquier, H., Mérola, F., Morel, N. & Erard, M. The enhanced cyan fluorescent protein: a sensitive pH sensor for fluorescence lifetime imaging. *Anal. Bioanal. Chem.* **405**, 3983–3987 (2013).
28. Linders, P. T. A., Ioannidis, M., Ter Beest, M. & Van Den Bogaart, G. Fluorescence Lifetime Imaging of pH along the secretory pathway. *ACS Chem. Biol.* **17**, 240–251 (2022).
29. Kimura, S., Noda, T. & Yoshimori, T. Dissection of the autophagosome maturation process by a novel reporter protein, tandem fluorescent-tagged LC3. *Autophagy* **3**, 452–460 (2007).

30. Asfari, M. et al. Establishment of 2-mercaptoethanol-dependent differentiated insulin-secreting cell lines. *Endocrinology* **130**, 167–178 (1992).

Acknowledgements
This work has received funding from the European Research Council (ERC) under the European Union's Horizon 2020 research and innovation programme (grant agreement No 866127, project CAPTUR3D). The PRIN 2022 BIZZARRI_2022RRFJC4 "Novel protein-based Genetically-Encoded Fluorescent Indicators (GEFI) for Functional Super-Resolution Imaging of Biomolecular Activities in Living Cells" – GEFinder. CUP I53D23003880006 from the Italian Ministry of University and Research is gratefully acknowledged.

Author contributions
V.D.L.: Conceptualization, Formal analysis, Investigation, Project administration, Visualization, Writing - original draft, writing - review & editing; S.G.: Formal analysis, Investigation, Visualization, writing - review & editing; M.B.: Data curation, Formal analysis, Visualization, writing - review & editing; G.M.: Formal analysis, Investigation; G.F.: Formal analysis, Investigation; B.S.: Investigation; R.B.: Conceptualization, Writing - original draft, writing - review & editing; F.C.: Conceptualization, Funding acquisition, Supervision, Writing - original draft, writing - review & editing.

Competing interests
The authors declare no competing interests.

Additional information
Supplementary information The online version contains supplementary material available at https://doi.org/10.1038/s42003-025-07758-w.

Correspondence and requests for materials should be addressed to Valentina De Lorenzi or Francesco Cardarelli.

Peer review information *Communications Biology* thanks Geert van den Bogaart and the other, anonymous, reviewer(s) for their contribution to the peer review of this work. Primary Handling Editor: Christina Karlsson Rosenthal. A peer review file is available.